Supplement of Atmos. Chem. Phys., 17, 13625–13644, 2017
https://doi.org/10.5194/acp-17-13625-2017-supplement

Atmospheric Chemistry and Physics
Open Access

Supplement of

Cloud climatologies from the infrared sounders AIRS and IASI: strengths and applications

Claudia J. Stubenrauch et al.

Correspondence to: Claudia J. Stubenrauch (stubenrauch@lmd.polytechnique.fr)

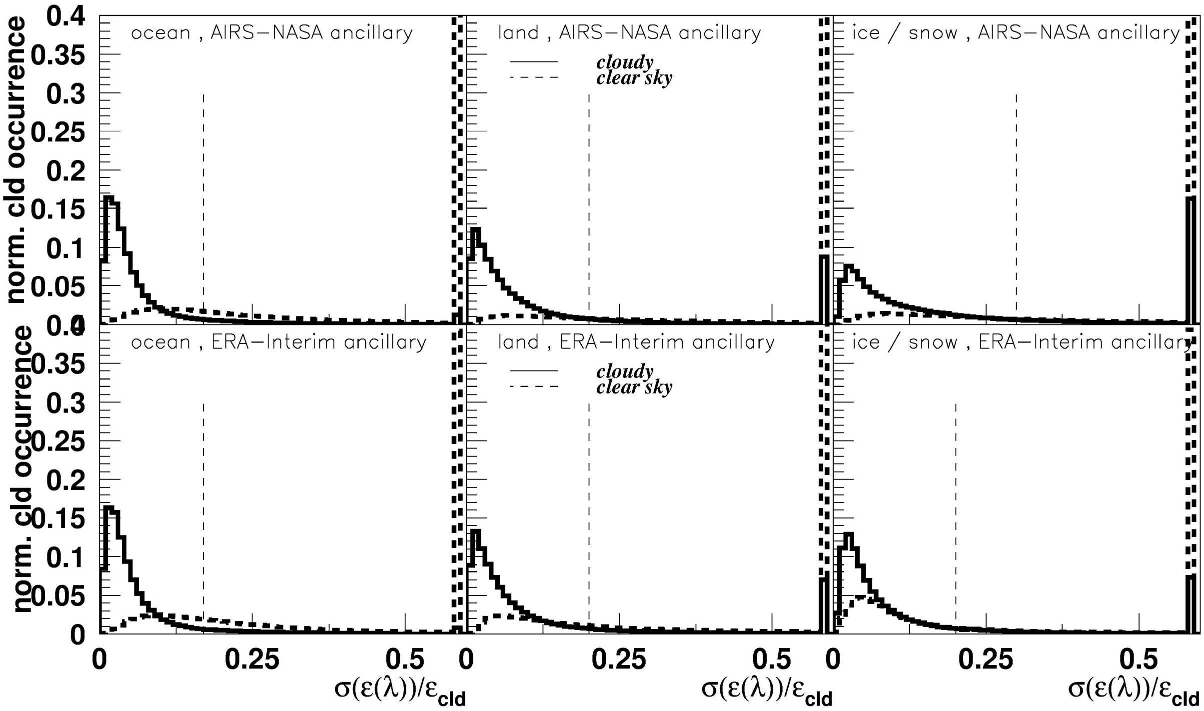

Figure S1. Normalized distributions of spectral variability of effective cloud emissivity over six wavelengths between 9 and 12 μm divided by cloud effective emissivity retrieved by the χ^2 method, separately for scenes declared as cloudy, and as clear sky. Statistics includes three years (2007-2009) of observations at 1:30AM LT, separately over ocean, over land and over ice / snow; top: with ancillary data deduced from AIRS-NASA and from ERA-Interim. Thresholds for cloud detection are indicated as dashed lines.

Cloudy includes at least one cloud layer from GEOPROF and from CALIPSO. Clear sky is defined by by three cloud-free CALIPSO samples within the AIRS golf ball.

These distributions are narrower for cloudy scenes than for clear sky, and they are very similar to those presented in Stubenrauch *et al.* (2010). The large tails of the distributions are folded into $\sigma(\varepsilon_\lambda)/\varepsilon_{cld}$, = 0.59, the maximum value to which $\sigma(\varepsilon_\lambda)/\varepsilon_{cld}$, was set. The separation between cloudy and clear is best over ocean, followed by land and then ice / snow. Distributions are similar over ocean and land between both ancillary data, whereas the distinction between cloudy and clear sky over ice / snow is slightly better when ERA-Interim is used. This might be explained by the fact that the retrieval of atmospheric profiles with good quality is challenging over ice / snow.

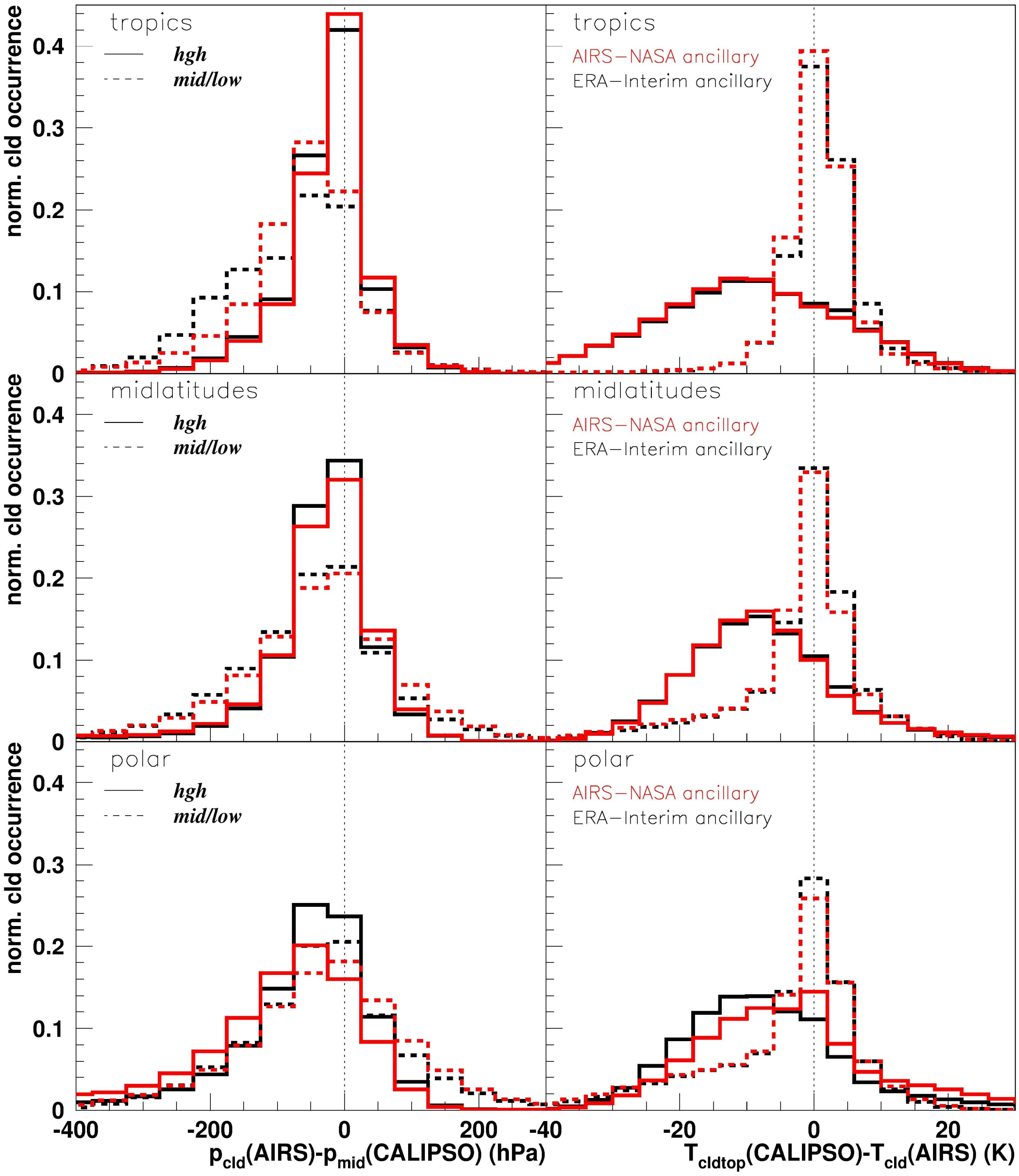

Figure S2. Normalized frequency distributions of the difference between the mid-cloud pressure (between the cloud top and the ‘apparent’ cloud height) from CALIPSO and p_{cld} from AIRS (left) and between the cloud top temperature from CALIPSO and T_{cld} from AIRS (right). Analysis over tropics (30°N-30°S), midlatitudes (30°-60°) and polar latitudes (60°-85°), separately for high-level clouds and for clouds with p_{cld} > 440 hPa. The effect of using different ancillary data is also presented. Statistics includes three years (2007-2009) of observations at 1:30AM LT.

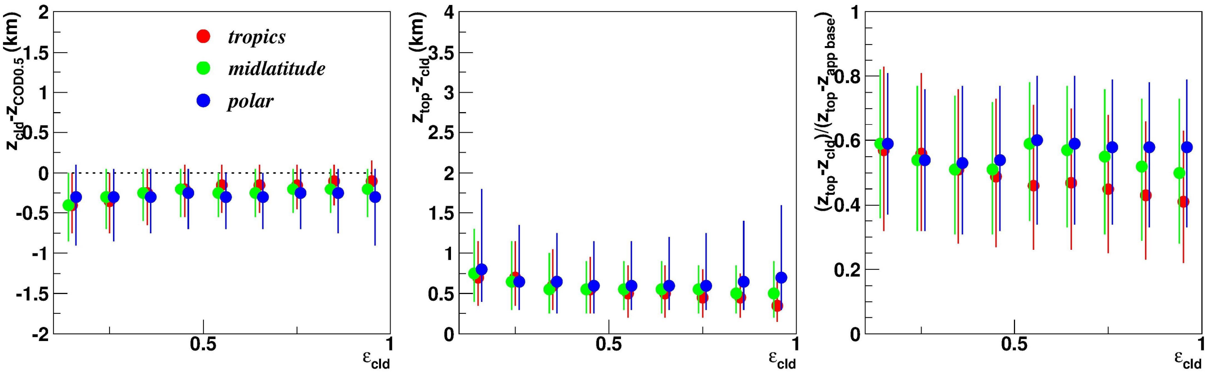

Figure S3. a) z_{cld} ï $z_{COD0.5}$, b) z_{top} - z_{cld} and c) (z_{top} - z_{cld}) / (z_{top} ï $z_{app\ base}$), as function of ε_{cld} for low-level clouds in the tropics, midlatitudes and polar latitudes. Presented are median values and the interquartile ranges. Three years of statistics, for which z_{cld} and $z_{COD0.5}$ lie within vertical cloud borders from GEOPROF. Observations at 1:30AM LT.

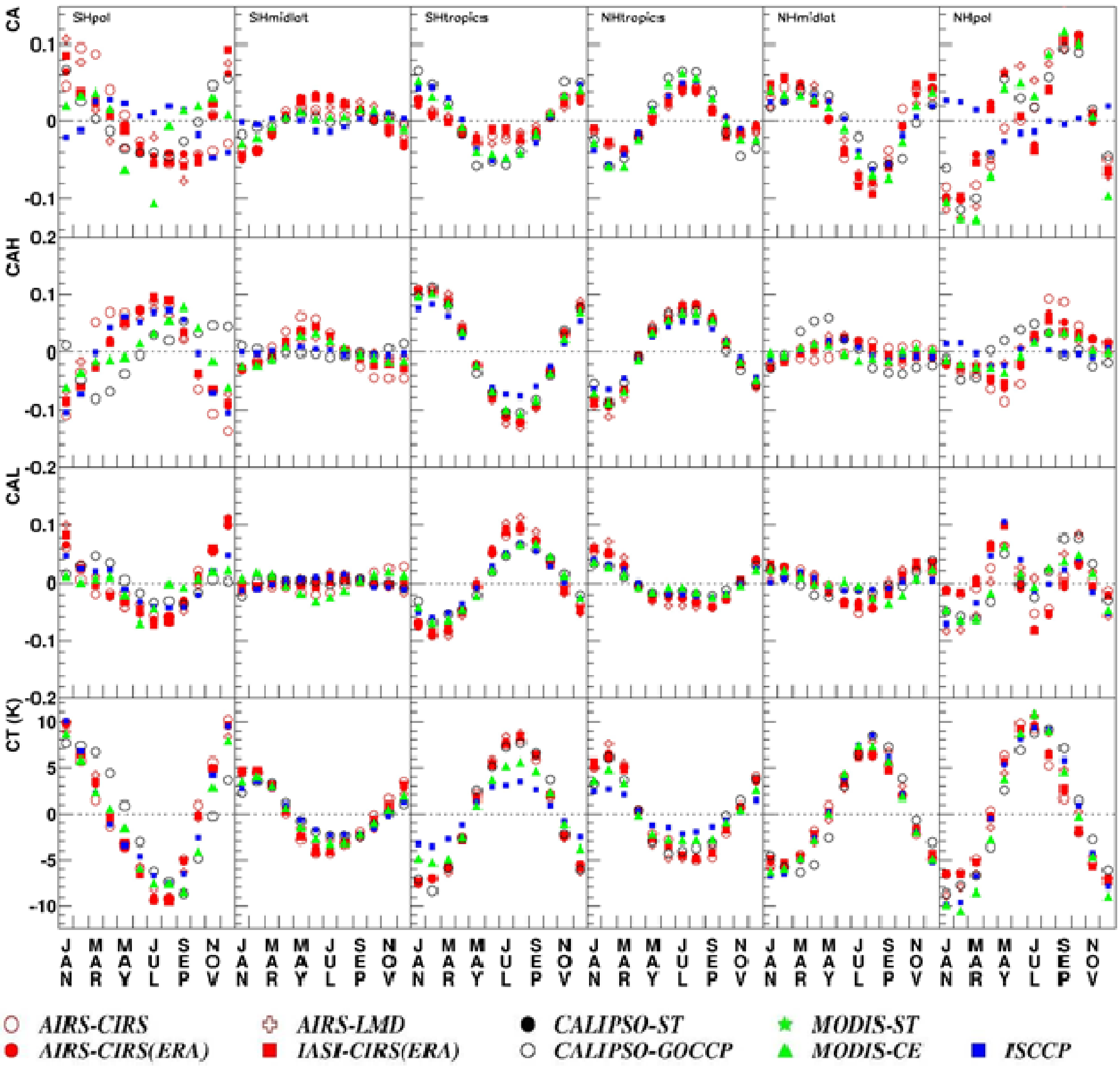

Figure S4. Seasonal cycle of CA, CAH, CAM, CAL and CT over 30° wide latitude bands from SH polar to NH polar.

As already acknowledged during the GEWEX Cloud Assessment (Stubenrauch *et al.*, 2013), the seasonal cycles agree quite well between the different data sets, with exception of the polar regions where passive remote sensing does not perform well and the active CALIPSO data do not have the same sampling as the other data sets in the GEWEX Cloud Assessment data base, because they exclude measurements from 1:30PM during polar night (polar winter) and from 1:30AM during polar day (polar summer).

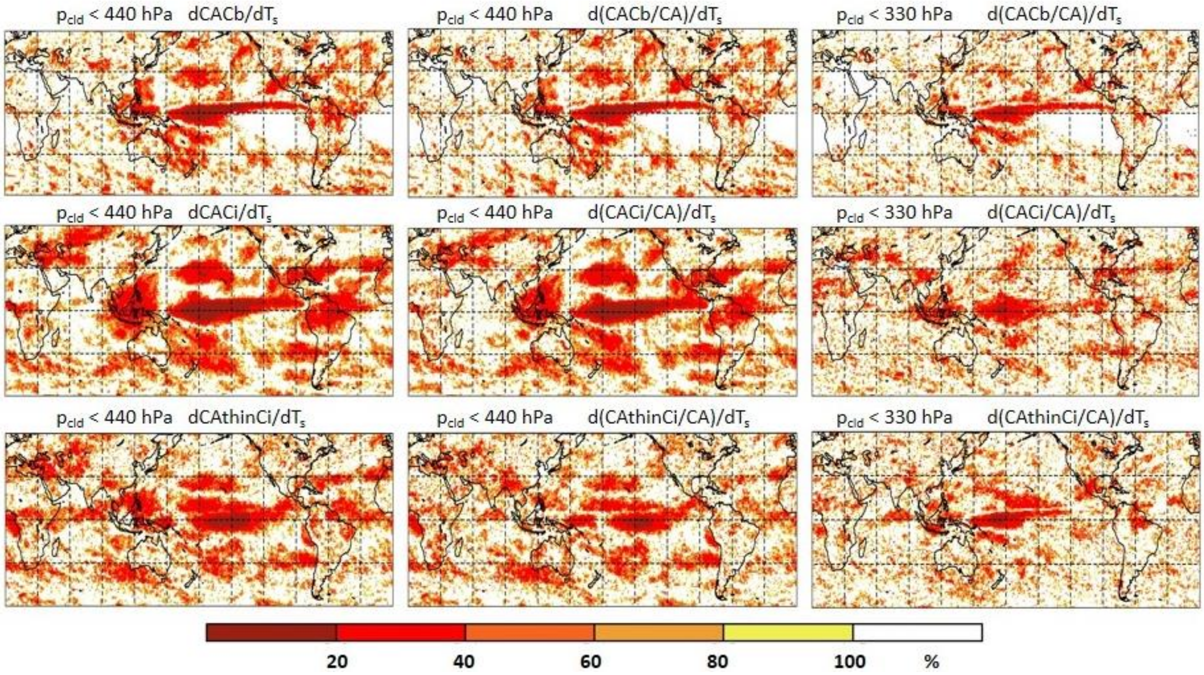

Figure S5. Geographical maps of relative slope uncertainty for linear regressions between monthly mean anomalies in amount of Cb (ε_{cld} > 0.95, top row), cirrus (0.95 > ε_{cld} > 0.4, middle row) and thin cirrus (0.4 > ε_{cld} > 0.1, bottom row) from AIRS-CIRS and global mean surface temperature anomalies from ERA-Interim; considering left: p_{cld} < 440 hPa, middle: relative cloud amount, right: p_{cld} < 330 hPa and relative cloud amount. Results using 156 months during the period 2003-2015.